

Document made available under the Patent Cooperation Treaty (PCT)

International application number: PCT/GB05/001280

International filing date: 01 April 2005 (01.04.2005)

Document type: Certified copy of priority document

Document details: Country/Office: GB
Number: 0407531.3
Filing date: 02 April 2004 (02.04.2004)

Date of receipt at the International Bureau: 13 June 2005 (13.06.2005)

Remark: Priority document submitted or transmitted to the International Bureau in compliance with Rule 17.1(a) or (b)



World Intellectual Property Organization (WIPO) - Geneva, Switzerland
Organisation Mondiale de la Propriété Intellectuelle (OMPI) - Genève, Suisse



INVESTOR IN PEOPLE

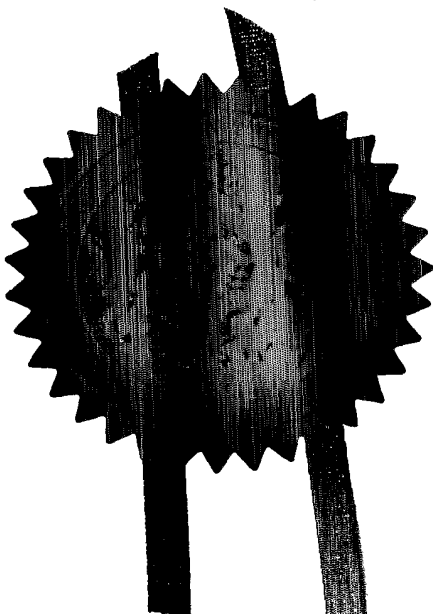
The Patent Office
Concept House
Cardiff Road
Newport
South Wales
NP10 8QQ

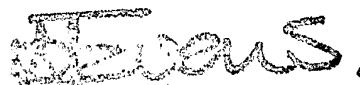
I, the undersigned, being an officer duly authorised in accordance with Section 74(1) and (4) of the Deregulation & Contracting Out Act 1994, to sign and issue certificates on behalf of the Comptroller-General, hereby certify that annexed hereto is a true copy of the documents as originally filed in connection with the patent application identified therein.

In accordance with the Patents (Companies Re-registration) Rules 1982, if a company named in this certificate and any accompanying documents has re-registered under the Companies Act 1980 with the same name as that with which it was registered immediately before re-registration save for the substitution as, or inclusion as, the last part of the name of the words "public limited company" or their equivalents in Welsh, references to the name of the company in this certificate and any accompanying documents shall be treated as references to the name with which it is so re-registered.

In accordance with the rules, the words "public limited company" may be replaced by p.l.c., plc, P.L.C. or PLC.

Re-registration under the Companies Act does not constitute a new legal entity but merely subjects the company to certain additional company law rules.



Signed 

Dated 18 May 2005



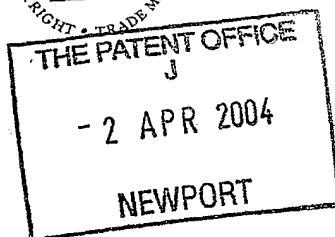
2 APR 2004



02APR04 E886035-1 002973
P01/7700 0.00-0407531.3 ACCOUNT CHA

Request for grant of a patent

(See the notes on the back of this form. You can also get an explanatory leaflet from the Patent Office to help you fill in this form)



The Patent Office

Cardiff Road
Newport
South Wales
NP10 8QQ

1. Your reference

MON/P104096GB

2. Patent application number

(The Patent Office will fill this part in)

0407531.3

3. Full name, address and postcode of the or of each applicant (underline all surnames)

Loughborough University
LOUGHBOROUGH
Leicestershire
LE11 3TU
GB

Patents ADP number (if you know it)

If the applicant is a corporate body, give the country/state of its incorporation

07280308002

4. Title of the invention

An Alloy

5. Name of your agent (if you have one)

Harrison Goddard Foote

"Address for service" in the United Kingdom to which all correspondence should be sent (including the postcode)

31 St Saviourgate
York
YO1 8NQ

Patents ADP number (if you know it)

07914237002 ✓

6. Priority: Complete this section if you are declaring priority from one or more earlier patent applications, filed in the last 12 months.

Country

Priority application number
(if you know it)

Date of filing
(day / month / year)

7. Divisionals, etc: Complete this section only if this application is a divisional application or resulted from an entitlement dispute (see note d)

Number of earlier UK application

Date of filing
(day / month / year)

8. Is a Patents Form 7/77 (Statement of inventorship and of right to grant of a patent) required in support of this request?

Answer YES if:

Yes

- a) any applicant named in part 3 is not an inventor, or
- b) there is an inventor who is not named as an applicant, or
- c) any named applicant is a corporate body.

Otherwise answer NO (See note d)

9. Accompanying documents: A patent application must include a description of the invention. Not counting duplicates, please enter the number of pages of each item accompanying this form:

Continuation sheets of this form

Description	15	2
Claim(s)	4	
Abstract	--	
Drawing(s)	9	

10. If you are also filing any of the following, state how many against each item.

Priority documents

Translations of priority documents

Statement of inventorship and right to grant of a patent (Patents Form 7/77)

Request for a preliminary examination and search (Patents Form 9/77)

Request for a substantive examination (Patents Form 10/77)

Any other documents (please specify)

11. I/We request the grant of a patent on the basis of this application.

Signature(s) *Harrison Goddard Foote*

Date *1/4/04*

12. Name, daytime telephone number and e-mail address, if any, of person to contact in the United Kingdom

Michelle O'Neill

1 April 2004

01904 732 120

Warning

After an application for a patent has been filed, the Comptroller of the Patent Office will consider whether publication or communication of the invention should be prohibited or restricted under Section 22 of the Patents Act 1977. You will be informed if it is necessary to prohibit or restrict your invention in this way. Furthermore, if you live in the United Kingdom, Section 23 of the Patents Act 1977 stops you from applying for a patent abroad without first getting written permission from the Patent Office unless an application has been filed at least 6 weeks beforehand in the United Kingdom for a patent for the same invention and either no direction prohibiting publication or communication has been given, or any such direction has been revoked.

Notes

- If you need help to fill in this form or you have any questions, please contact the Patent Office on 08459 500505.
- Write your answers in capital letters using black ink or you may type them.
- If there is not enough space for all the relevant details on any part of this form, please continue on a separate sheet of paper and write "see continuation sheet" in the relevant part(s). Any continuation sheet should be attached to this form.
- If you have answered YES in part 8, a Patents Form 7/77 will need to be filed.
- Once you have filled in the form you must remember to sign and date it.
- Part 7 should only be completed when a divisional application is being made under section 15(4), or when an application is being made under section 8(3), 12(6) or 37(4) following an entitlement dispute. By completing part 7 you are requesting that this application takes the same filing date as an earlier UK application. If you want the new application to have the same priority date(s) as the earlier UK application, you should also complete part 6 with the priority details.

"An alloy"

This invention relates to a chromium alloy comprising hafnium. In particular it relates to steel comprising hafnium and a method for preparing said steel.

In recent years, much interest has been paid to the development of new alloys which would be suitable for the application in super-critical power plants. One of the methods to improve the creep property is to add micro-alloying elements. There have been a number of such kinds of study using both experimental observations and computer modelling (1, 2). For example, studies have shown that micro-additions of zirconium improve the creep resistance of chromium steels and decrease the oxidation rate sharply (3, 4). It also reduces the depletion of chromium from grain boundaries due to irradiation (5). Vodarek and Strang studied the effects of Ni on the precipitation process in a 12CrMoV steels during creep at 550 °C and found that when the content of Ni exceeds about 0.6 wt.%, the creep properties of the material will drop considerably (6).

Many studies have been carried out on the effects of hafnium on the microstructure and properties of super-alloys. Kim *et al.* found that addition of hafnium and carbon to a Nb-Mo-W alloy results in the formation of (Nb, Mo, Hf)C. The yield stress at 1773 K and fracture toughness at room temperature increase concurrently with increasing content of (Hf+C) in the alloy (7). Garg *et al.* found that small additions of Hf to conventionally processed NiAl single crystals result in the precipitation of a high density of cuboidal G-phase particles with size from 5 to about 50 nm ($1\text{nm} = 10^{-9}\text{ m}$) (8).

There are as yet no known methods of using hafnium directly in the production of chromium alloys such as steel. An object of the present invention is, therefore, to provide further processes for the improvement and production of chromium alloys, such as steel.

According to a first aspect of the present invention there is provided a chromium alloy comprising hafnium.

In a preferred aspect of the invention, the chromium alloy is steel. More preferably, the steel is a stainless steel such as ferritic grade steel.

In power plant ferritic steels, high volumes of finely distributed stable second phase particles are desirable to improve the creep properties of the material at high temperature and stress. By studying the effects of hafnium on the microstructure of ferritic steels using ion implantation and modelling it has, surprisingly, been found that the invention results in a steel in which a larger number of small hafnium rich particles was formed. The steel prepared according to the invention has been found to have improved creep properties as well as an increased chromium content and thus improved corrosion resistance

Attempts have been made to increase the chromium content of chromium containing ferritic steels by directly adding more chromium into a 12% chromium ferritic steel. It was found that the microstructure of the steel began to transform to delta ferrite when the chromium content of the steel rose above 12% (Schneider. H, Foundry Trade J., 108: p. 562 (1960)). Since the alloy relies on the formation of martensite for its strength, the dilution of the martensite by the delta ferrite rapidly lead to a loss in strength of the overall alloy.

The chromium alloy may comprise up to 1 atomic(at)%, for example, up to 0.5 at% hafnium.

The chromium alloy may comprise an atomic% of carbon up to 1%, for example up to 0.5% or up to 0.4%. The hafnium may react with the carbon in the alloy to form hafnium carbide which may be in the form of hafnium carbide particles. Preferably, the hafnium, or hafnium carbide, is provided in the surface of the alloy of the

invention. Thus the invention provides a chromium alloy in which hafnium is in the outer 1-2 μ m of the alloy i.e. in the surface of the alloy.

Preferably, the chromium alloy of the invention is free of particles of $M_{23}C_6$ wherein M is an alloy of chromium with small amounts of molybdenum and iron. More preferably, the alloy of the invention comprises particles of M_2N .

The alloy of the invention may comprise less than 12wt% chromium, for example, less than 10wt% chromium such as 8 or 9wt% chromium.

The alloy may contain one or more of the elements selected from Groups 3 to 16, for example, one or more of the elements selected from Groups 3 to 12. Typically, the alloy contains one or more elements selected from aluminium, molybdenum, titanium, carbon, silicon, manganese, phosphorous, sulphur, nickel, vanadium, niobium, tungsten and nitrogen. Preferably, the alloy of the invention comprises vanadium, niobium, molybdenum and nitrogen.

In a further aspect, the present invention provides a supercritical power plant comprising an alloy according to the invention. As used herein a "supercritical power plant" is intended to include, but is not limited to, a boiler operating at temperatures above 565°C.

Hafnium may be added to the steel during casting or moulding of the steel.

Alternatively, powders of iron, chromium, hafnium and optionally other alloying elements may be mixed together and mechanically alloyed. The resulting powder may be then sealed in argon-containing or vacuum tight containers and then may be hot isostatically pressed and sintered at high temperature (e.g 200 C) before being extruded into rod or bar form.

In a further aspect, the present invention provides a method for the manufacture of steel, the method comprising the steps of:

- (i) addition of hafnium to steel;
- (ii) heat treating the steel formed in step (i).

Preferably, the hafnium is added to steel by implantation into the steel. In a preferred embodiment of the invention, the hafnium is added to steel by ion implantation. This method has the advantage in that it allows the hafnium to dispersed homogeneously in the steel in relatively large concentrations.

The present inventors have found that in order to reduce intragranular corrosion of steel, it is sufficient to implant the hafnium in the surface of the steel. This surface modification preferably takes place in the outer 1-2 μm of the steel using ion implantation.

The heat treatment step preferably takes place at a temperature of 700-760°C. This tempering treatment may take 1 to 2 hours and may be followed by a cooling of the tempered steel

In a preferred method of the invention, up to 1.0 at% hafnium is added to the steel, for example, up to 0.5 at% hafnium.

Preferably the steel is a chromium alloy, for example, a stainless steel. The stainless steel may be ferritic grade steel. The steel may comprise less than 12wt% chromium, for example, less than 10wt% chromium such as 8 or 9wt% chromium. The steel may contain one or more of the elements selected from Groups 3 to 16, for example, one or more of the elements selected from Groups 3 to 12. Typically, the steel will contain one or more elements selected from aluminium, molybdenum, titanium, carbon, silicon, manganese, phosphorous, sulphur, nickel, vanadium, niobium, tungsten and nitrogen. Preferably, the steel comprises vanadium, niobium, molybdenum and nitrogen.

Preferably, the method of the invention is for the manufacture of steel suitable for use in a super critical power plants.

In a further aspect, the invention provides a method for the introduction of hafnium into steel characterised in that the hafnium is added directly to the steel by ion implantation.

A yet further aspect of the invention provides the use of hafnium in the manufacture of steel. The steel may be stainless steel such as ferritic grade steel.

In a further aspect, the invention provides steel obtainable by the method of the invention.

The present invention will now be described by way of example only with reference to the accompanying figures, wherein:

Figure 1. Microstructures of E911 (a) at the as-received condition and (b) after tempering at 760 °C for 1 hour.

Figure 2. Spectrum of the grain boundary precipitates in raw E911.

Figure 3. EDX spectrum of the MX particles: (a) V rich; (b) Nb rich.

Figure 4 TEM image of the microstructure of E911 with ~1 at.% hafnium implantation after tempering at 760 °C for 1 hour.

Figure 5. TEM image showing densely distributed small precipitates in Hf implanted E911 samples.

Figure 6. Amount of equilibrium phases present in (a) raw E911 and (b) Hf implanted E911 material.

Figure 7. Mole fraction of different elements in (a) FCC and (b) HCP_A3 phases in the Hf implanted E911 material calculated using MTDATA.

Figure 8. EDX Spectrum of small precipitates in the E911 samples with hafnium implantation after tempering at 760 °C for 1 hour.

Figure 9. EDX spectrum of larger precipitates in E911 samples with hafnium implantation after tempering at 760 °C for 1 hour.

Figure 10. Electron diffraction pattern from a small particle rich area.

Figure 11. Electron diffraction patterns from larger particles in Hf implanted E911 samples. Same (h, k, l) values are labelled in the image.

Figure 12 Equivalent circle diameter measured from TEM images as a function of the implantation level.

Figure 13. Measured precipitate area fraction as a function of the implanted hafnium level.

Figure 14. Precipitation curves predicted (lines) for M_2N , HfC in the Hf implanted E911 and VN in the raw material. Symbols are measurements at the end of tempering. Circle: M_2N ; Square HfC; Triangle: VN.

Figure 15. Predicted creep curves considering the coarsening effects of second phase particles for HfC and M_2N in the Hf implanted and for VN in the raw E911 material. The temperature is 600 °C and stress is 150 MPa.

Example

Materials

The material used in this work is a 9 wt.% Cr ferritic steel, E911. The chemical composition of the material is shown in Table 1. The material was supplied by Corus at the as-received condition, *i.e.* normalised at 1060°C for 1 hour then air cooled. Thin foils for TEM examination were cut and polished from the as-received material without any further treatment.

Ion implantation

Ion implantation was carried out at Hokkaido University, Japan. The machine used was the ULVAC 400 kV Ion Accelerator. The hafnium target used for the implantation were manufactured by the Institute of Pure Chemicals, Japan. The purity of the hafnium target is 99.99%. The ion current was kept at about 1 μA (10^{-6} Amperes). The samples then were implanted for 30 and 60 minutes. These two levels of implantation is roughly equivalent to 0.5 and 1.0 at.% of Hf implantation.

Tempering and TEM

The thin foils implanted with hafnium were then tempered at 760 °C for 1 hour using the in-situ furnace in the high voltage TEM machine, JEM-ARM1300 at Hokkaido University, Japan. The samples were heated to the tempering temperature for around five minutes, and then kept at this temperature for 1 hour. After cooling down in the furnace, TEM pictures of the microstructure of the samples were then taken for the measurement of particle size and volume fraction using the image analysis software, Image-Pro Plus. Compositional determination of the particles were carried out using the FEI Tecnai F20 Field Emission Gun Transmission Electron Microscope. Electron diffraction patterns were taken using JEOL JEM 100CX TEM.

Results and discussion

Microstructure of the material without addition of hafnium

The microstructure of the as-received material is shown in Fig. 1(a). As expected, the as-received material shows a clear lath structure without any profound evidence of precipitation. The width of the laths is a few hundred nanometres. After tempering, two kinds of precipitates formed. One is mainly located at the grain boundaries with the elongated axis along the grain boundaries, and the others are mainly in the matrix and are with spherical morphology and they are much smaller than the grain boundary precipitates (see Fig. 1(b)). The EDX spectrum of the grain boundary particles is shown in Fig. 2. It is clear that the grain boundary precipitates are a chromium rich phase, though the spectrum is influenced by the matrix composition. Therefore, it is concluded that they are $M_{23}C_6$ particles which are found in most ferritic steels and are located mainly at grain boundaries. It is also clear that there is a small amount of molybdenum in these grain boundary precipitates.

The smaller, and intra-granular particles are thought to be MX particles as in most ferritic steels. Two types of MX particles were found in the tempered E911 samples. These EDX spectra are shown in Fig. 3. In one type of the particles, there is a sound evidence of the presence of vanadium. In recognising that the spectrum is very likely to be much noise by the matrix and that the distortion by the matrix is more severe in the case of small particles, we are confident that these are VN or V(C,N) particles. In the other type of small particles, there is a clear indication of a high content of vanadium. However, the content of niobium in these particles is much higher than that of vanadium. Therefore, these are (Nb, V) C or (Nb, V) (C,N) precipitates. These observations are in very good agreement with reports in the literature (8).

Microstructure of the material with implantation of hafnium

The microstructure of the hafnium implanted E911 after tempering at 760 °C for 1 hour is shown in Fig. 4. The difference between the microstructure of the Hf implanted and raw E911 samples is clear. Firstly, here there are an enormous number of small particles, as clearly shown in Fig. 5. Secondly, the larger particles are not

only along grain boundaries, but can be found in the matrix as well. Therefore, it is concluded that some kind of new phase maybe formed with the implantation of Hf as compared to the raw material.

MTDATA calculations.

In order to determine the phases present in the Hf implanted material, MTDATA (10, 11) was used to determine the equilibrium phases. Fig. 6 shows the calculated amount of different phases present in both (a) the raw material and (b) the Hf implanted material, as a function of temperature. At the tempering temperature employed in this study, *i.e.* 1033 K, there are mainly three phases in the raw material, they are α -Fe, $M_{23}C_6$ and VN. This is in very good agreement with experimental observations as discussed above. Comparing Fig. 6(b) with (a), the $M_{23}C_6$ phase has disappeared. Instead, a new phase, HCP_A3 presents. This phase can exist to a higher temperature than $M_{23}C_6$. Another FCC phase is also present, but it is not VN any more, because its dissolution temperature is much high than that of VN.

The composition of the FCC phase according to MTDATA as a function of temperature is shown in Fig. 7(a). The atomic fraction of Hf is 0.5 at the tempering temperature and is nearly a constant at different temperatures. The atomic fraction of carbon varies from 0.33 to 0.43 and has a value of 0.37 at the temperature employed in this study. The phase also contains from 0.07 to 0.17 atomic fraction of vacancies. These atomic fraction values clearly suggest that the FCC phase is HfC with a substantial fraction of the carbon sites unoccupied. This also explains the disappearance of $M_{23}C_6$ particles from the Hf implanted material. Because the high amount of Hf implanted (0.5 to 1.0 at.%) and the carbon content in the material is much lower than that of Hf, all carbon is taken by Hf to form HfC. This supports the observation that that Hf is a stronger carbide former than Cr.

Fig. 7(b) shows the composition of the HCP_A3 phase as a function of temperature. It is clear that phase mainly contains Cr, V, Nb, Mo and N. The atomic fraction of N is about 1/3. Therefore, this new phase has a composition of M_2N , which is similar to

the commonly known Z-phase (CrNbN) (12). The difference is that Z-phase has a tetragonal rather than hexagonal structure. We believe that this phase is a variant of the Cr_2N phase which also has a hexagonal crystal structure. However, as the Z-phase is not included in the databases used in MTDATA, we can not exclude the possibility that this phase is the Z-phase. It is also clear that there are few VN particles because most of the nitrogen has been taken by the new M_2N phase.

EDX studies

The composition of the particles present in the Hf implanted E911 material was also studied using TEM. A typical EDX spectrum taken from small particles in the material is shown in Fig. 8. As it can be seen from the figure, there is clear evidence for the presence of Hf in these small particles. Because the particles are very small (diameter less than 10 nm), the spectrum contains a very high contribution from the matrix. From this, we can conclude that the small particles in the material are Hf rich.

Fig. 9 shows an example of the EDX spectrum from the larger particles present in the Hf implanted E911 samples. The content of Cr in these particles is much lower than that in M_{23}C_6 particles in the raw material (cf. Fig. 2). This indicates that these particles are most probably not M_{23}C_6 precipitates. It is also clear that the larger particles do not contain an appreciable amount of Nb, as is the case in the Z-phase. Thus the larger particles may be not the Z-phase.

In summary, EDX studies show that there is a fine Hf rich phase and a distribution of larger precipitates which are not M_{23}C_6 particles present in the Hf implanted material. This is in a very good agreement with the MTDATA calculations discussed in the previous section.

Electron diffraction patterns

Electron diffraction patterns from the small particles are very difficult to take, because they are below the equipment's resolution limit. Therefore, diffraction patterns were taken from areas where there are many small particles, such as the area

shown in Fig. 5. An example is shown in Figure 10. Due to the diffraction from the matrix and other particles, the diffraction pattern is very noisy and it is very difficult to identify the spots corresponding to specific phases. However, it is also clear that there is some sort of ring structure in the pattern. X-ray standard diffraction data for HfC was used to fit the corresponding d -values from the pattern shown in Fig. 10. It was found that most of the d -values listed in the X-ray diffraction data for HfC can be matched. In combination with the results from EDX analysis and MTDATA calculations, it is concluded that the small particles present in the Hf implanted E911 material are HfC.

Electron diffraction patterns from the larger particles in Hf implanted E911 samples are shown in Fig. 11. Because the size of the particles is much larger (~ 65 nm in diameter) than HfC particles, the diffraction patterns are cleaner. A similar approach to that of determining the structure of HfC particles was taken. Table 2 lists the d values of $(\text{Cr,Fe})_2\text{N}_{1-x}$ from x-ray diffraction, compared with d values found from electron diffraction patterns obtained in this study. Clearly, all the values of d listed in the diffraction data card are matched reasonably well, especially the strongest lines are matched very well. The electron diffraction patterns from the larger particles are also analysed against diffraction data of Z-phase, as shown in Table 3. It is clear that a substantial proportion of the d values listed in the standard x-ray diffraction data card have not been matched. In addition, these un-matched d values include a few of the strong diffraction lines from x-ray diffraction. Therefore, it is more likely that these larger particles are hexagonal M_2N rather than Z-phase. Considering the fact that the EDX from these particles does show an appreciable amount of Nb, as it is the case in Z-phase (CrNbN), we conclude that the larger particles in Hf implanted E911 material are hexagonal M_2N .

From above discussions, it is clear that Hf has very significant effects on the microstructure of E911 material. Firstly it prevents the formation of the M_{23}C_6 particles present in the raw materials by forming a FCC structured HfC, which takes most of the carbon in the material. According to our creep modelling calculations,

$M_{23}C_6$ coarsens very fast and thus accelerates creep damage considerably. From this point of view, the removal of $M_{23}C_6$ by the formation of HfC is very beneficial for the creep properties of the material. Secondly, two new phases are formed: HfC and M_2N . Because most of the nitrogen has been taken by the M_2N phase, there are few VN particles. Because of the smaller size of the M_2N compared to that of $M_{23}C_6$ particles in the raw materials (~90 nm in diameter) and because M_2N is distributed everywhere rather than mainly along grain and lath boundaries, it is believed that M_2N would be better for the creep properties of the material than $M_{23}C_6$. HfC is expected to have similar behaviour to VN. However, as the volume fraction of HfC (~1.9%) is much higher than that of VN in the raw material (~0.3%), it may also lead to improvements in the creep behaviour of the material.

Another important effect of Hf on the microstructure of E911 is that it will increase the Cr content in the matrix and thus at the grain boundaries. From the volume fractions of M_2N in the Hf implanted material and of $M_{23}C_6$ in the raw material and the Cr content in those two phases, it can be calculated that the matrix content of Cr would increase by about 1 at.% when $M_{23}C_6$ is replaced by M_2N due to the addition of Hf. This would improve the corrosion resistance property of the material considerably.

Effects of hafnium implantation on precipitate size and volume fraction

As discussed above, the implantation of hafnium introduced a large number of very small particles in the material. Therefore, it has a considerable effect on the overall average size and volume fraction of the particles. Figs. 12 and 13 show the effect of the hafnium implantation level on the average precipitate size and volume fraction.

The average particle size was measured as the equivalent circle diameter, *i.e.* the diameter of a circle with the same area. The level of implantation is presented as implantation time with 1 hour is roughly equivalent to 1.0 at.% of implantation. It is clear that the addition of hafnium reduces the average size of the precipitates considerably, because of the formation of a large number of smaller hafnium rich

particles. The higher the concentration of hafnium, the smaller the average particle size. However, the reduction in particle size when the implantation level exceeds 0.5 at.% is less marked. The overall reduction of average particle size is more than 50%.

The volume fraction of the precipitates was measured as the area fraction of the particles. It is easy to understand that this may not be the representation of the true volume fraction of the particles in the material as here we are sampling a volume of the material. However, the area fraction is an indicator of the true volume fraction of the particles. The area fraction of the particles is presented in Fig. 13 as a function of implantation time. It is clear that the addition of hafnium increases the total volume fraction of the precipitates considerably.

It is believed that a substantial volume fraction of fine distributed second phase particles would improve the creep behaviour of power plant ferritic steels at high temperatures. From Figs. 12 and 13, it is concluded that the addition of hafnium to power plant ferritic steels would achieve this.

Precipitation and Creep behaviour of HfC and M_2N

In order to look at the long term effect of the two new phases created by the introduction of Hf into the E911 material, precipitation kinetics of both new phases were simulated using our newly developed model (13, 14), the effect of these phases on the creep behaviour was modelled using the Continuum Creep Damage Mechanics (CDM) model¹⁵ and the results were compared with that of VN in the raw material.

Fig. 14 shows the predicted precipitation kinetics of M_2N and HfC particles in the Hf implanted E911 material, tempered at 760 °C for 1 hour then aged at 600 °C for up to 1000,000 hours. To facilitate comparison, the predicted precipitation curve of VN in the raw E911 material with the same heat treatment conditions, is also presented. Symbols are experimental measurements of the particle size at the end of tempering. Generally speaking, the model predictions agree with the measurements. Both HfC

and M_2N coarsen faster than VN in the raw material. This is because that both phases have much higher volume fraction than VN, thus smaller inter-particle spacing. Therefore, the diffusion of solute atoms between the particles is easier. Nevertheless, for the same reason, the material with HfC and M_2N has better creep behaviour than that with VN particles within the normal life time scale of the material as predicted using CDM modelling. This is clearly shown in Fig. 15, where predicted creep curves for all the three types of particles are shown.

Conclusions

The implantation of hafnium to E911 has significant effects on the microstructure of Fe-9Cr steel. Hafnium enters a new precipitate phase, which is very finely distributed hafnium carbide with spherical shape. The particle density of the hafnium carbide is huge. $M_{23}C_6$ particles which normally exist in power plant steels are not present in the Hf implanted material, due to most of the carbon atoms being taken by the hafnium carbide. This indicates that Hf can prevent the formation of $M_{23}C_6$ particles. Instead of the chromium rich phase $M_{23}C_6$, a new chromium rich hexagonal phase, M_2N , forms in the Hf implanted material. These particles have diameters of about 65 nm and are distributed homogeneously in the material rather than along the grain boundaries. The replacement of $M_{23}C_6$ particles by the M_2N phase increases the matrix chromium level by nearly 1 at.%, resulting in an increase in the corrosion resistance of the implanted material. Implantation of Hf to E911 results in a marked decrease in the overall average size of the precipitates and a increase in the volume fraction of the second phase particles. The long term precipitation behaviour of the two new phases is similar, but coarsening faster than VN in the raw material. However, their presence will improve the material's creep behaviour significantly as predicted by the CDM modelling due to their much higher volume fraction as compared to VN.

References

1. H. Okada, S. Muneki, K. Yamada, H. Okubo, M. Igārashi, and F. Abe: *ISIJ INTERNATIONAL*, 2002, **42**, 1169-1174.

2. Y. F. Yin, and R. G. Faulkner: *Materials Science and Engineering A*, 2003, **344**, 92-102.
3. A. V. Ryabchenkov, V. A. Tarzhumanova , and S. A. Yuganova: *Materials Science and Heat Treatment*, 1985, **27**, 756-759.
4. V. A. Repin, L. I. Shvedov, G. V. Volkov, and V. V. Suprunenk: *STEEL IN THE USSR*, 1991, **21**, 237-239.
5. N. Shigenaka, S. Ono, Y. Isobe, T. Hashimoto, H. Fujimori, and S. Uchida: *Journal of Nuclear Science and Technology*, 1996, **33**, 577-581.
6. V. Vodarek, and A. Strang: *SCRIPTA MATERIALIA*, 1997, **38**, 101-106.
7. W. Y. Kim, H. Tanaka, M. S. Kim, and S. Hanada: *Materials Science and Engineering A*, 2003, **346**, 65-74.
8. A. Garg, R. D. Noebe, and R. Darolia: *Acta Materialia*, 1996, **44**, 2809-2820.
9. P. J. Ennis, and A. Czyrska-Filemonowicz: *OMMI*, 2002, **1**, 1-28.
10. R. H. Davies *et al.*, *Proc. Conf. ASM/TMS Fall meeting on 'Applications of thermodynamics in the synthesis and processing of materials'*, Rosemont, IL, USA, Oct 1994, 371-384.
11. R. H. Davies, A. T. Dinsdale, T. G. Chart, T. I. Barry, and M. H. Rand: *High Temperature Science*, 1990, **26**, 251-262.
12. T. Sourmail: *Materials Science and Technology*, 2001, **17**, 1-14.
13. Y. F. Yin, and R. G. Faulkner: *Materials Science and Technology*, 2003, **19**, 91-98.
14. Y. F. Yin, and R. G. Faulkner: In '*Power Technology*', (ed. J. Lecomte-Beckers *et al.*), Vol. 21, 1247-1256; 2002, Jülich: Forschungszentrum Jülich GmbH.
15. B. Dyson: *Journal of Pressure Vessel Technology*, 2000, **122**, 281-296.

CLAIMS

1. A chromium alloy comprising hafnium.
2. A chromium alloy as claimed in claim 1 comprising up to 1 atomic% hafnium.
3. A chromium alloy as claimed in claim 2 comprising up to 0.5 atomic% hafnium.
4. An alloy according to any of claims 1 to 3 that is steel.
5. An alloy according to claim 4 that is stainless steel.
6. An alloy according to claim 5 that is ferritic grade steel.
7. An alloy as claimed in any of claims 1 to 6 wherein the hafnium is in the form of hafnium carbide.
8. An alloy as claimed in any of claims 1 to 7 wherein the hafnium is in the outer 1-2 μ m of the alloy.
9. An alloy according to any preceding claim comprising less than 12wt% chromium.
10. An alloy according to claim 9 comprising less than 10wt% chromium.
11. An alloy according to any preceding claim which contains one or more of the elements selected from Groups 3 to 16 of the periodic table.

12. An alloy according to claim 11 which contains one or more of the elements selected from Groups 3 to 12.
13. An alloy according to claim 12 wherein the elements are selected from aluminium, molybdenum, titanium, carbon, silicon, manganese, phosphorous, sulphur, nickel, vanadium, niobium, tungsten and nitrogen.
14. An alloy according to claim 13 comprising vanadium, niobium, molybdenum and nitrogen.
15. A supercritical power plant comprising an alloy as claimed in any of claims 1 to 14.
16. A method for the manufacture of steel, the method comprising the steps of:
- (i) addition of hafnium to steel;
 - (ii) heat treating the steel formed in step (i).
17. A method as claimed in claim 16 wherein the steel is a chromium alloy.
18. A method as claimed in claim 17 wherein the steel is stainless steel.
19. A method as claimed in claim 18 wherein the steel is ferritic grade steel.
20. A method as claimed in any of claims 16 to 19 wherein the steel contains up to 10 wt% chromium.
21. A method as claimed in any of claims 16 to 20 wherein the steel alloy contains one or more of the elements of Groups 3 to 16.

22. A method as claimed in claim 21 wherein the steel alloy contains one or more of the elements of Groups 3 to 12.

23. A method as claimed in claim 21 or 22 wherein the steel alloy contains one or more of aluminium, molybdenum, titanium, carbon, silicon, manganese, phosphorous, sulphur, nickel, vanadium, niobium, tungsten and nitrogen.

24. A method as claimed in any of claims 16 to 23 wherein the hafnium is implanted in the steel.

25. A method as claimed in any of claim 24 wherein the hafnium is added by ion implantation.

26. A method as claimed in claim 25 wherein the ion implantation is applied to the surface layer of the steel.

27. A method as claimed in claims 24 to 26 wherein the hafnium is implanted in the outer 1-2 μm surface of the steel.

28. A method as claimed in any of claims 16 to 27 wherein up to 1.0 at% hafnium is added to the steel.

29. A method as claimed in claim 28 wherein up to 0.5 at% hafnium is added to the steel.

30. A method as claimed in any preceding claim wherein the steel is heat treated in step (ii) to a temperature of 700-760°C.

31. A method as claimed in claim 30 wherein the heat treatment is for 1 to 2 hours.

32. A method for the manufacture of steel suitable for use in super critical power plants as claimed in any of claims 16 to 31.
33. A method for the introduction of hafnium into steel characterised in that the hafnium is added directly to the steel by ion implantation,
34. Use of hafnium in the manufacture of steel.
35. Use as claimed in claim 34 wherein the steel is stainless steel.
36. Use as claimed in claim 35 wherein the steel is ferritic grade steel.
37. Steel obtainable by the method of any of claims 16 to 33.
38. Steel or a method as substantially hereinbefore described.

Table 1 Chemical composition of E911 (wt.%, Fe balance)

C	Si	Mn	P	S	Cr	Mo	Ni	V	Al	Nb	W	N
0.115	0.19	0.35	0.007	0.003	9.10	1.00	0.22	0.23	0.006	0.069	0.98	0.069

Table 2 X-ray diffraction data of HfC compared with the d values found from the electron diffraction patterns obtained here.

Data from X-Ray diffraction card			Matched	Error
d/Å	I/I ₁	hkl	d/Å	(%)
2.68	100	111		
2.321	90	200	2.33	0.39
1.641	70	220	1.645	0.25
1.399	80	311	1.396	-0.22
1.340	30	222	1.32	-1.5
1.160	10	400	1.17	0.87
1.065	50	331	1.06	-0.47
1.038	50	420		
0.9473	40	422	0.960	1.4
0.8932	50	333,511		
0.8204	30	440		
0.7845	80	531		
0.7735	70	600		

Table 3 X-ray diffraction data of (Cr,Fe)₂N_{1-x} compared with the d values found from the electron diffraction patterns obtained here.

Data from X-Ray diffraction card			Matched	Error (%)
d/Å	I/I ₁	hkl	d/Å	
2.399	16	110	2.3572	-1.8
2.233	40	002	2.174	-2.7
2.114	100	111	2.1191	0.25
1.634	35	112	1.639	0.31
1.387	25	300	1.399	0.87
1.266	30	113	1.264	-0.16
1.178	20	302	1.174	-0.34
1.159	16	221	1.174	1.3
1.115	10	004	1.081	-3.1
1.054	8	222	1.081	2.6
1.013	8	303	1.002	-1.1
0.9342	35	223	0.9336	-0.07

Table 4 X-ray diffraction data of Z-phase (CrNbN) compared with the d values found from the electron diffraction patterns obtained here.

Data from X-ray diffraction card			Matched		
d /Å	I/I ₁	hkl	d /Å	Error (%)	
7.380	1	001			
3.650	3	002			
2.803	8	101	2.779	-0.9	
2.461	25	003			
2.344	55	102	2.357	0.6	
2.144	40	110	2.152	0.4	
2.051	1	111	2.098	2.3	
1.913	18	103	1.899	-0.8	
1.853	3	112	1.890	2.0	
1.847	15	004	1.840	-0.4	
1.618	40	113	1.639	1.3	
1.578	10	104	1.566	-0.8	
1.518	35	200	1.554	2.4	
1.491	1	201			
1.478	18	005			
1.403	1	202	1.399	-0.4	
1.400	30	114	1.399	-0.1	
1.336	17	211	1.399	4.7	
1.329	55	105			
1.292	40	203			
1.275	100	212			
1.231	7	006			
1.218	65	115	1.174	-3.7	
1.189	40	213	1.174	-1.3	
1.175	50	204	1.174	-0.1	

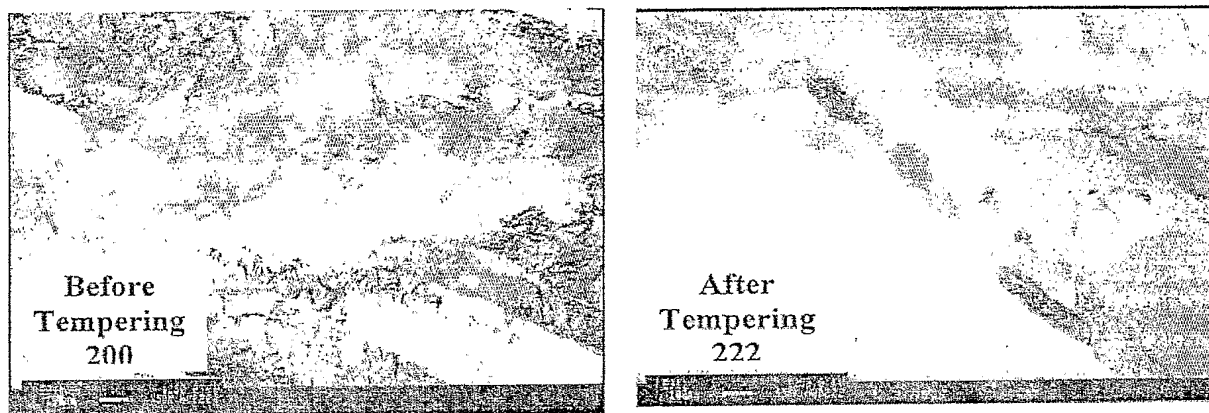


Figure 1. Microstructures of E911 at the as-received condition and after tempering at 760 °C for 1 hour.

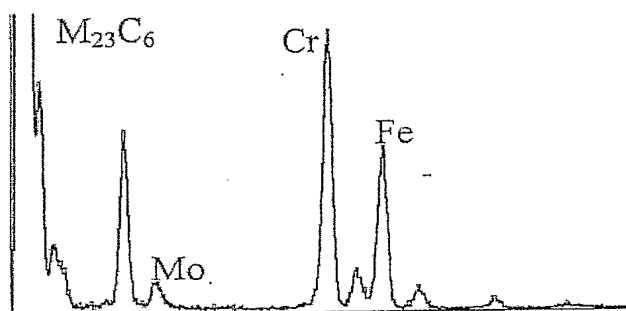


Figure 2. Spectrum of the grain boundary precipitates in raw E911.

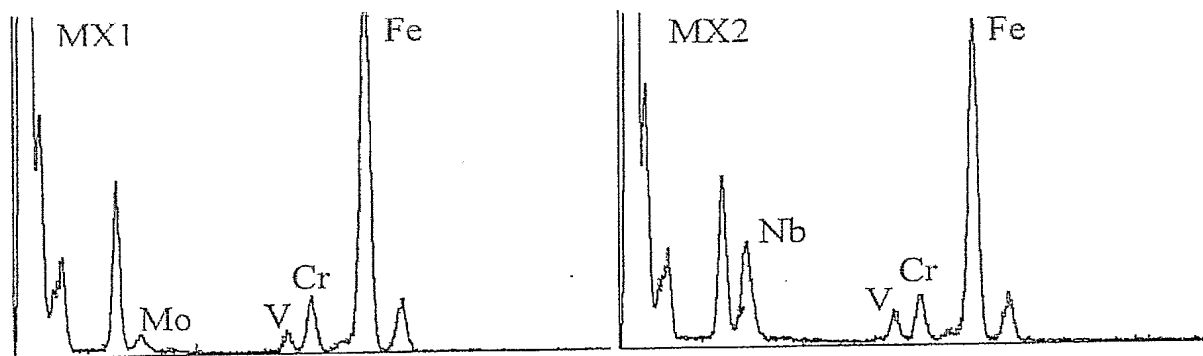


Figure 3. EDS spectrum of the MX particles.



Figure 4 TEM image of the microstructure of E911 with ~1 at.% hafnium implantation after tempering at 760 °C for 1 hour.

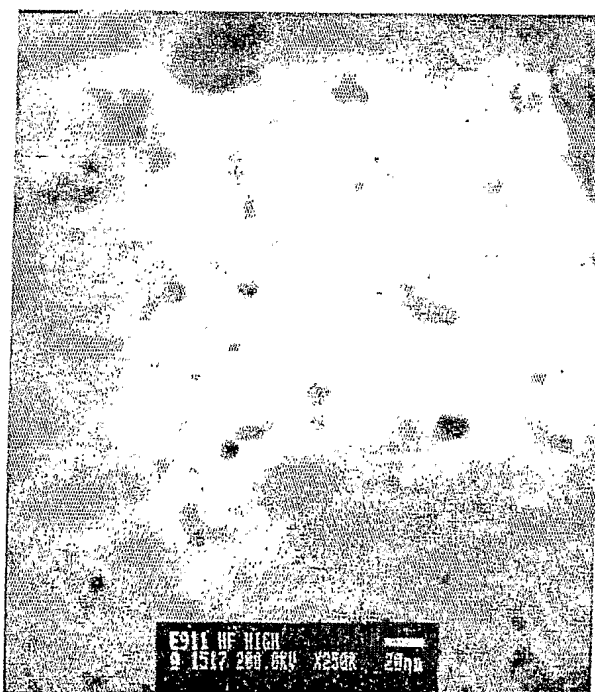


Figure 5. TEM image showing densely distributed small precipitates in Hf implanted E911 samples.

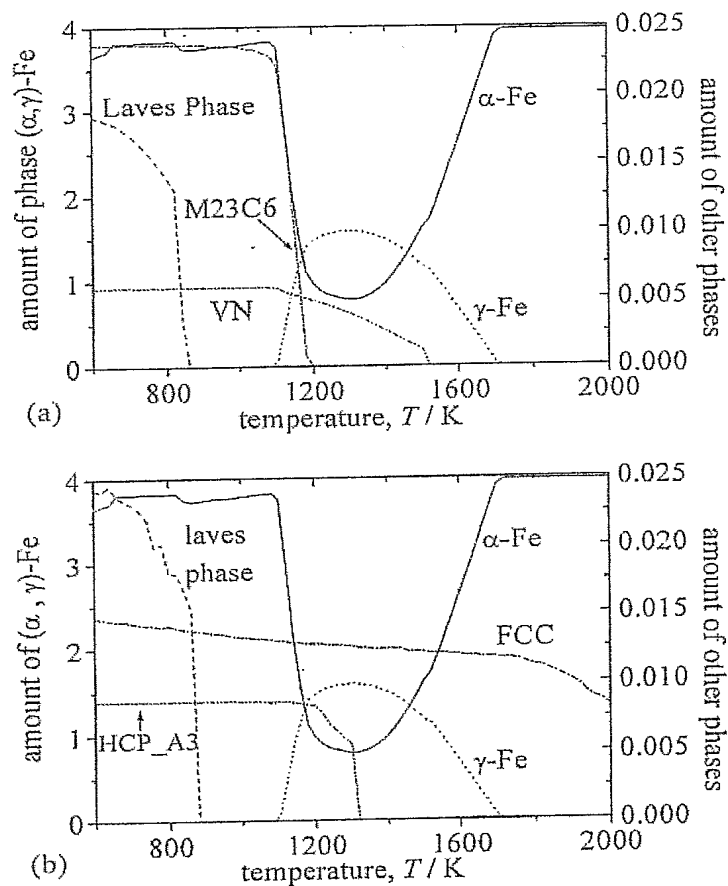


Figure 6. Amount of equilibrium phases present in (a) raw E911 and (b) Hf implanted E911 material.

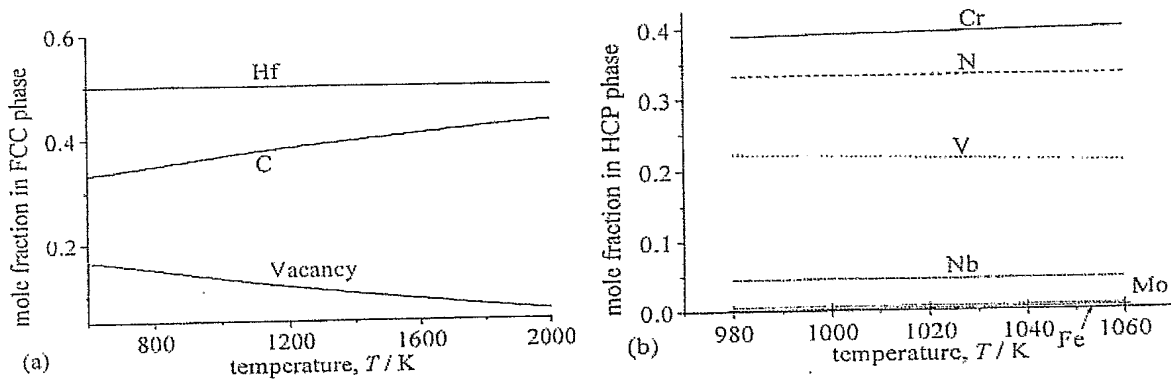


Figure 7. Mole fraction of different elements in (a) FCC and (b) HCP_A3 phases in the Hf implanted E911 material calculated using MTDATA.

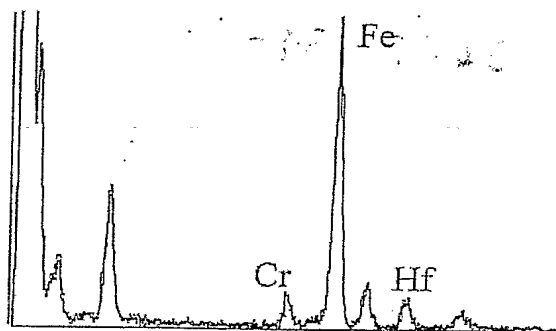


Figure 8. EDX Spectrum of small precipitates in the E911 samples with hafnium implantation after tempering at 760 °C for 1 hour.

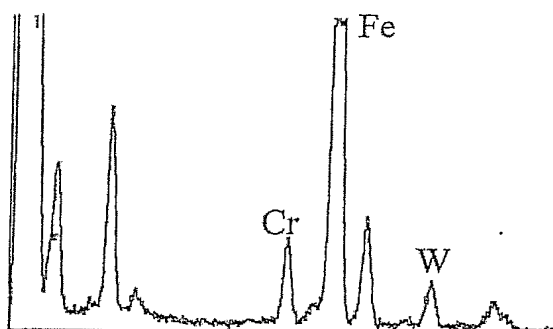


Figure 9. EDX spectrum of larger precipitates in E911 samples with hafnium implantation after tempering at 760 °C for 1 hour.

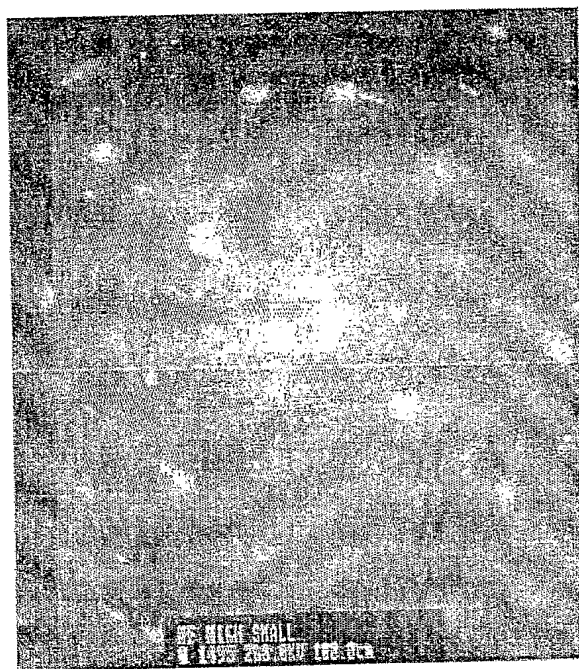


Figure 10. Electron diffraction pattern from a small particle rich area.

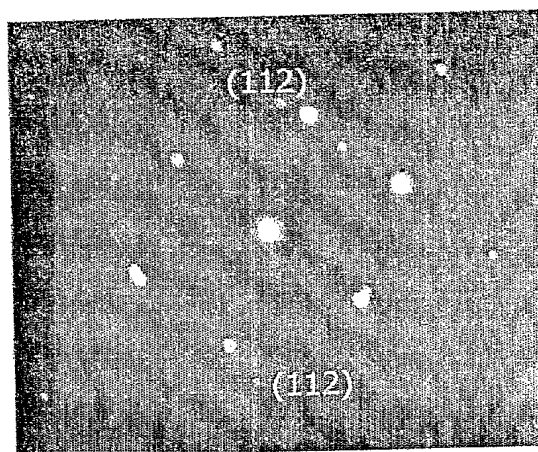
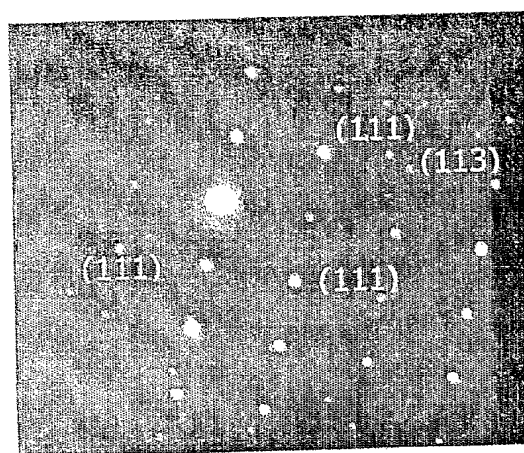


Figure 11. Electron diffraction patterns from larger particles in Hf implanted E911 samples. Same (h, k, l) values are labelled in the image.

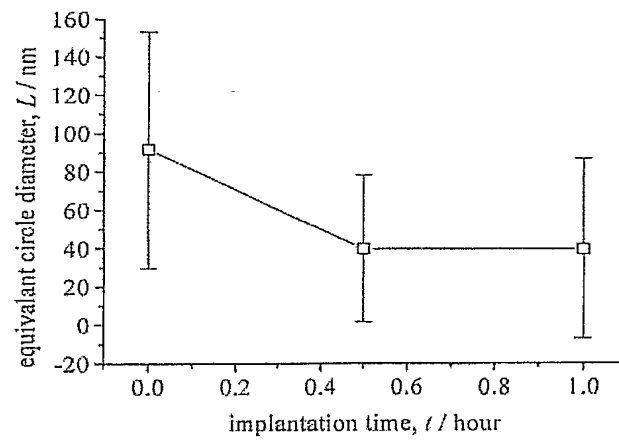


Figure 12 Equivalent circle diameter measured from TEM images as a function of the implantation level.

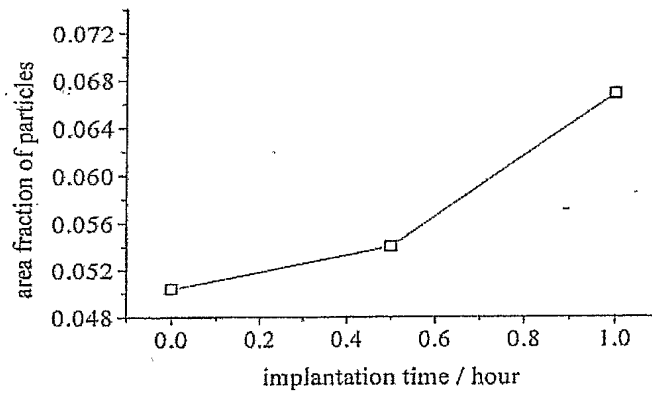


Figure 13. Measured precipitate area fraction as a function of the implanted hafnium level.

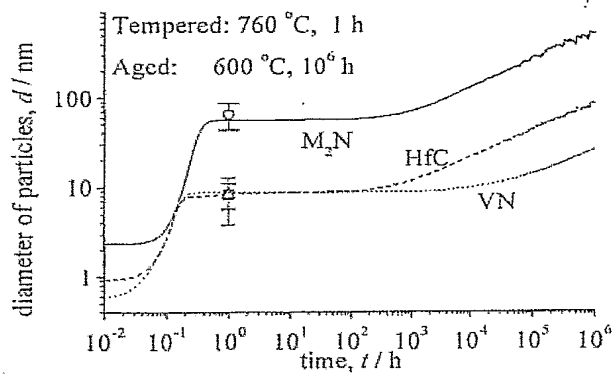


Figure 14. Precipitation curves predicted (lines) for M_2N , HfC in the Hf implanted E911 and VN in the raw material. Symbols are measurements at the end of tempering. Circle: M_2N ; Square HfC; Triangle: VN.

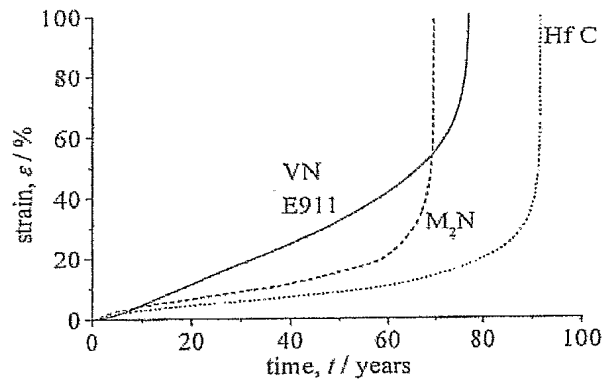


Figure 15. Predicted creep curves considering the coarsening effects of second phase particles for HfC and M_2N in the Hf implanted and for VN in the raw E911 material. The temperature is 600 °C and stress is 150 MPa.



